

X-ray fluorescence sorting of non-ferrous metal fractions from municipal solid waste incineration bottom ash processing depending on particle surface properties

Kerstin Pfandl¹ , Bastian Küppers¹ , Stefanie Scheiber², Gerhard Stockinger³, Johannes Holzer⁴, Roland Pomberger¹, Helmut Antrekowitsch² and Daniel Vollprecht¹

Abstract

A heavy non-ferrous metal fraction (<50 mm) of municipal solid waste incineration bottom ashes from wet-mechanical treatment was separated by screening, magnetic separation and eddy-current separation into ferrous metals, non-ferrous metals and residual sub-fractions. The non-ferrous metal fractions were divided and subjected to (i) a washing process, (ii) dry abrasion and (iii) no mechanical pre-treatment to study the effect of resulting different surface properties on a subsequent X-ray fluorescence sorting into precious metals, zinc, copper, brass, stainless steel and a residual fraction. The qualities of the X-ray fluorescence output fractions were investigated by chemical analyses (precious metal fraction and the residual fraction), pyrometallurgical tests and subsequent chemical analyses of the metals and slags produced by the melting processes (zinc, copper, brass and stainless steel fraction). Screening directs brass and stainless steel primarily into the coarser fractions, while copper and residual elements were rather transferred into the finer fractions. X-ray fluorescence sorting yielded zinc, copper, brass, stainless steel and precious metals fractions in marketable qualities. Neither a negative nor a positive impact of mechanical pre-treatment on the composition of these fractions was identified. Solely the yield of the brass fraction in the grain size 16–20 mm decreased with increasing mechanical pre-treatment. The pre-treatment also had no impact on yield and quality of the products of pyrometallurgical tests.

Keywords

Bottom ash, X-ray fluorescence sorting, metal recovery, mechanical processing, surface properties, municipal solid waste incineration residues, metal recycling, heavy non-ferrous metals

Introduction

The number of municipal solid waste incineration (MSWI) plants increases worldwide. Since 2015, more than 200 new plants with an overall annual capacity of more than 50 million tonnes have been put into operation. By the end of 2017, 2450 plants, with a capacity of 330 million tonnes per year, were operating, of which the majority (about 75%) are grate furnace plants, about 20% are fluidised bed plants and about 5% run on alternative technologies (ecoprogramm GmbH, 2018).

In grate furnace plants, between 150 and 250 kg MSWI bottom ash per tonne of input material are produced (Kranert and Cord-Landwehr, 2010). Normally, MSWI bottom ash is discharged via a water bath. The water content of wetly discharged bottom ash accounts for about 20 wt% (Simon and Holm, 2013). Bottom ash contains, besides (earth) alkaline metals, chlorides, silicates and sulphates, ferrous and non-ferrous metals and metal compounds. The mineral fraction adds up to 85–90 wt%, the

metals (scrap) 7–10 wt% and the residues (not or only partly combusted) 1–5 wt% (Gillner et al., 2011). The main constituents of the metal fraction are iron, aluminium, copper, brass and stainless steel (Bunge, 2016). Furthermore, bottom ash contains a number of critical raw materials according to the definition of the European Commission (2017), for example rare earth elements,

¹Chair of Waste Processing Technology and Waste Management (AVAW), Montanuniversität Leoben, Leoben, Austria

²Chair of Nonferrous Metallurgy (NEM), Montanuniversität Leoben, Leoben, Austria

³Brantner Gruppe GmbH, Krems an der Donau, Austria

⁴REDWAVE a division of BT-Wolfgang Binder GmbH, Eggersdorf bei Graz, Austria

Corresponding author:

Kerstin Pfandl, Chair of Waste Processing Technology and Waste Management (AVAW), Montanuniversität Leoben, Franz Josef-Str. 18, 8700 Leoben, Austria.

Email: kerstin.pfandl@unileoben.ac.at

antimony, vanadium, cobalt, gallium, tungsten, niobium, tantalum, beryllium, germanium, indium, rhodium, palladium, ruthenium (ordered according to the average contents) in MSWI ashes in descending order according to Pfandl et al. (2018), Allegrini et al. (2014), Bayuseno and Schmahl (2010), Funari et al. (2015), Johnson and Huter (2010), Jung and Osako (2007), BOKU (2010) and Zhang et al. (2001) and phosphorus (Pan et al. 2008; Wang et al. 2016). Although, copper and zinc are not defined as critical raw material, they have a high economic importance compared with other raw materials according to the European Commission (2017). Furthermore, zinc is considered as potentially critical raw material in Austria (Bundesministerium für Verkehr, Innovation und Technologie, 2018).

MSWI bottom ashes are mostly subjected to mechanical processing in order to recover at least the metals and partly also to recycle the mineral fraction. Although the composition of bottom ash is similar in different geographic regions, no two processing plants are identical. Even plants in the same region and accordingly with the same legislation often use different technologies, which suggests that there is still optimisation potential in bottom ash processing (Bunge, 2016).

According to Bunge (2014, 2016), the value of the potentially recoverable metals accounts for approximately €60 per tonne of bottom ash. Owing to increasing raw material prices, the separation of metals provides benefits not only from an environmental, but also from a financial point of view. Besides energy savings, compared with the mining of primary raw materials, the primary raw material consumption and accompanied waste generation during production can be reduced (Simon and Holm, 2013).

The processes for separation of metallic and mineral constituents of bottom ash are comparable with those that are used in mineral processing of primary raw materials. The disagglomeration of metal–mineral intergrowths (sintering) can be achieved by comminution, for example by impact mills (Simon and Holm, 2013). An alternative technology, which offers potential for further research, is electrodynamic fragmentation (Dittrich et al., 2016). The classification of bottom ash is conducted by using different screens, for example bar sizer, drum screen and flip-flop screen (Bunge, 2016). Ferrous metals are normally separated by magnetic separators of different design, non-ferrous metals by eddy-current separators (Gillner et al., 2011). In mechanical processing plants, jigs are used to enrich material groups based on density separation in different output flows (Pfandl et al., 2018). A dry-mechanical alternative to swim-sink-separation is density separation via X-ray transmission (XRT) (Gisbertz and Friedrich, 2015).

Sensor-based sorting is increasingly used for the sorting of non-ferrous metals (e.g. copper, brass, stainless steel). The potential suitability of X-ray fluorescence (XRF) sorting in bottom ash processing has been demonstrated several times (Gisbertz and Friedrich, 2015; Kollegger and Berghofer, 2017). XRF, though, is limited to the particle surface and especially for bottom ash processing, the influence of surface defilements must be considered (Gisbertz and Friedrich, 2015). These can be significantly

impacted by factors, such as mechanical stress during the processing steps. However, currently there is no meaningful scientific information on the influence of particle surface properties of bottom ash on the XRF sorting efficiency.

Thus, in this study, a set of experiments was conducted to investigate the impact of different mechanical treatment procedures and resulting particle surface properties on the XRF sorting efficiency. Obtained results serve as a basis for an optimised sorting and thereby may lead to an increased recycling of bottom ash.

Materials and methods

Waste origin and sampling

Among others, the company Brantner operates a wet-mechanical bottom ash processing plant that uses the Brantner Wet Slag (BWS) process, presented in Figure 1.

In the first step, oversized pieces are removed via pre-screening at mesh size 50 mm and subsequently magnetic constituents are separated by an overbelt magnet. The core aggregate of the BWS process is a jig that splits the bottom ash into four fractions: (1) a swimming fraction (e.g. plastics, paper and textiles), (2) a heavy non-ferrous (HNF) fraction (e.g. non-ferrous metals, precious metals and stainless steel), (3) a light fraction (e.g. minerals and aluminium) and (4) a sludge fraction. From the light fraction (3), an aluminium and a non-ferrous metals concentrate is produced by eddy current separation with previous magnetic separation of ferrous metals. The separation of the HNF metals in the grain size range 0.02–2 mm (5) is realised in the Fine Slag Treatment Plant (FSTP). The fractions ‘magnetic bottom ash’ and ‘bottom ash’, as well as the ‘sludge’ from jiggling, are currently landfilled.

Each year about 40,000 t of waste incineration bottom ash is processed in the BWS process. For the experiments, the HNF metals from the jig and the FSTP (grain size 0–50 mm; ~0.5 wt% of the plant input) were chosen as the sample material. Sampling was conducted based on ÖNORM S 2127 (Österreichisches Normungsinstitut, 2011) and yielded a sample weight of about 2 t.

The conducted work is summarised in Figure 2 and described in detail in the following.

Mechanical processing

To prepare the HNF metals 0–50 mm for XRF sorting, the sample was subdivided into grain sizes of 0–6.3 mm, 6.3–10 mm, 10–16 mm, 16–20 mm and 20–50 mm in batch mode using the following screen types and linings.

- Waste screen Type SM 800×2450 FV, IFE Aufbereitungstechnik GmbH, standard mesh, mesh size 20 mm;
- Waste screen Type SM 800×2450 FV, IFE Aufbereitungstechnik GmbH, finger screen lining, mesh size 16 mm;
- Flip-flop screen ST 800×3600 F, IFE Aufbereitungstechnik GmbH, screen mat, mesh size 10 mm.

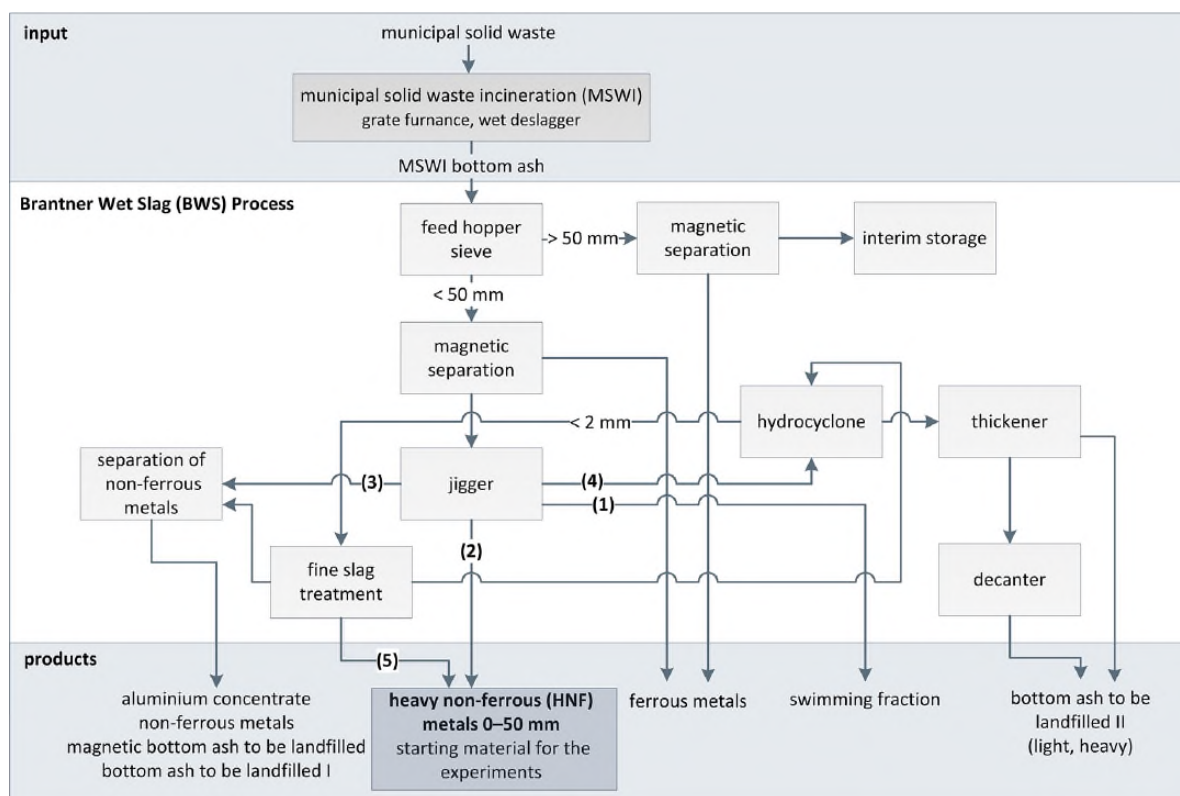


Figure 1. Brantner Wet Slag (BWS) process – modified and updated after Pfandl et al. (2018) and Stockinger (2016).

- Screen UE 500×1330 FSV LM645T, IFE Aufbereitungstechnik GmbH, screen lining, mesh size 6.3 mm.

Material feeding was conducted via feeding trays. Magnetic constituents of the produced grain size fractions 6.3–10 mm, 10–16 mm and 16–20 mm were separated using a drum magnet (HPG 500×650/13, barium ferrite magnets, brimming feeding), non-ferrous metals (NF fractions) by eddy current separation (INPXS 650×500/36). Owing to the grain size limits of the REDWAVE sorter used (see *XRF sorting*), the grain size fractions 0–6.3 mm and 20–50 mm were not further processed.

Surface pre-treatment

For the study of the influence of particle surface treatment on the XRF sorting result, the NF fractions 6.3–10 mm, 10–16 mm and 16–20 mm from mechanical processing were divided into three parts (i) surface treatment, dry, (ii) surface treatment, wet and (iii) no surface treatment. The pre-treatment was conducted batch-wise (maximum 80 kg) in a commercial concrete mixer (ATIKA BM 125 S). During dry-mechanical processing, the material remained in the mixer under continuous stirring for 20 min. For the wet-mechanical processing, 9 L water was added after 15 min of dry stirring. After a further 5 min of rotating, the water was discharged and another 9 L of water was added. The entire content of the drum was discharged and the water was collected separately.

XRF sorting

Altogether nine NF fractions (6.3–10 mm: (i) dry, (ii) wet, (ii) not pre-treated; 10–16 mm: (i) dry, (ii) wet, (ii) not pre-treated and 16–20 mm: (i) dry, (ii) wet, (ii) not pre-treated) with a total mass of 442 kg were sorted via XRF sorting in batch mode (REDWAVE 1350 XRF chute, sorting width 450 mm with X-ray tube and detectors). The material was discharged with 12 valves and 48 nozzles via compressed air.

Precious metals (gold, silver, palladium, platinum), zinc, copper and brass were separated as ejects subsequently in the respective order (positive sorting), namely the reject of the first run were fed again to the sorter and the subsequent eject was separated in the next run, etc. (first run: ejection of precious metals, reject fed again to the sorter, second run: ejection of copper, . . .). For the separation of a stainless steel fraction, the method of negative sorting was applied, namely all particles were ejected containing elements that are not allocated to the stainless steel fraction (last run). The working steps described above were repeated for the six NF fractions 10–16 mm and 16–20 mm. Owing to the small amounts of stainless steel present in the three NF fractions 6.3–10 mm (shown by previous analyses), only precious metals, zinc, copper and brass were separated from the fractions in this grain size range.

The detection of metals was conducted at the following energies of characteristic X-rays: copper: 8.05 keV; zinc: 8.64 keV; gold: 9.71 keV; silver: 22.16 keV; palladium: 21.18 keV; platinum: 9.44 keV. The following minimum contents constitute the

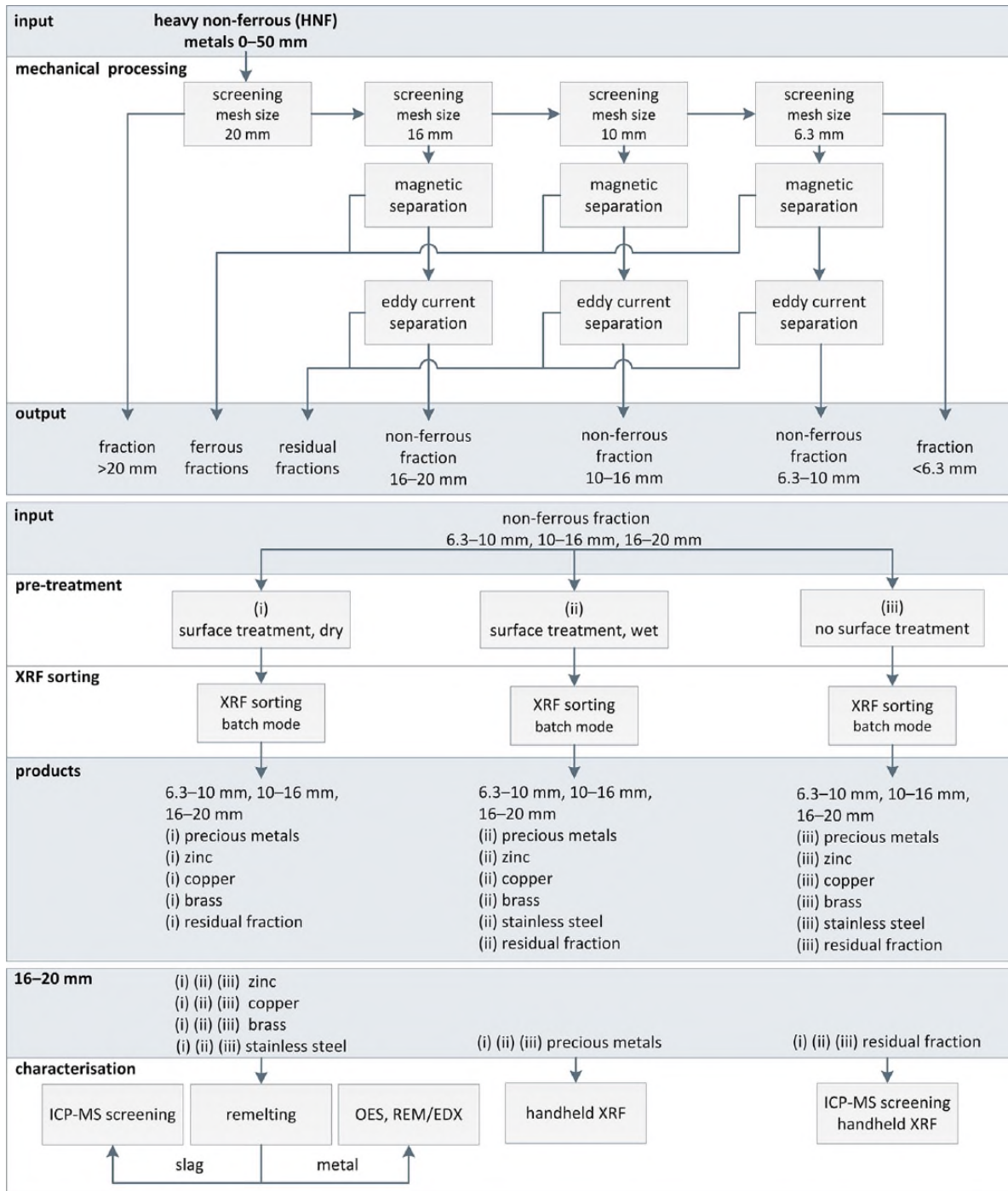


Figure 2. Conducted work, overview on methodology.

thresholds for the allocation of a particle to a fraction: copper >85%; zinc >85%; brass: copper >60% zinc >20%; precious metals: >1%.

Melting tests

In order to homogenise the chemical composition of XRF sorting products, two samples of each fraction in the range of 16–20 mm (zinc, copper and stainless steel) were remolten in an induction furnace (Indutherm MU 700). The used input weights amounted to 1500 g. Graphite crucibles were used for all experiments.

Additionally, a condenser was used to collect the evaporating elements and to determine their masses. The experimental temperature was chosen sufficiently high to melt the desired metal and sufficiently low to avoid the volatilisation of alloying elements, for example zinc from brass (550°C for zinc, 950°C for brass, 1150°C for copper and 1550°C for stainless steel). The holding period for zinc and copper melts accounted for 30 min and aimed for the dissolution of accompanying elements in the metal phase. The brass and stainless steel fractions were kept at the desired temperature for 10 min to avoid excessive volatilisation of zinc and to keep the erosion of the crucible and the combustion of

graphite low. The slags were skimmed from the metal melt. The respective metal was first cast in suitable sample shapes for subsequent analyses, the remaining metal melt was cast into bar shapes. The corresponding input fractions and the solidified melts and skimmed slags were weighed. Owing to their low weights and their inhomogeneity, the precious metal fractions were not remelted. However, their chemical composition was determined using a handheld XRF (see *Chemical analyses*).

Chemical analyses

The elemental composition of the remelted metal fraction (zinc, copper, brass, stainless steel) was determined by scanning electron microscopy using energy-dispersive X-ray spectroscopy (SEM/EDX, Jeol JSM-IT300) and via optical emission spectroscopy (OES, spark spectrometer SPECTROMAXx). Because of the good homogenisation owing to electromagnetic stirring in the induction furnace, only one sample of each melt was poured into a round steel mould. After metallographic preparation, including grinding with SiC papers of divers grain sizes and polishing with diamond suspension of 1 µm, the samples were analysed at three different areas using SEM/EDX analysis. Besides, OES analyses were applied at four different positions of each sample. From these values, the mean and the standard deviations were determined.

The slags from the melting experiments were processed (comminution with a jaw crusher, mortar and pestle to <2.5 mm, rejuvenation, homogenisation) and digested by aqua regia according to ÖNORM EN 13657(6.3) (Österreichisches Normungsinstitut, 2002b) or totally according to ÖNORM EN 13656 (Österreichisches Normungsinstitut, 2002a). Digested samples were analysed for silver, aluminium, gold, calcium, cobalt, chromium, copper, iron, potassium, magnesium, manganese, molybdenum, sodium, niobium, nickel, lead, palladium, platinum, antimony, silicon, tin, vanadium, tungsten and zinc by inductively coupled plasma mass spectrometry (ICP-MS screening, Agilent 7500ce) following ÖNORM EN ISO 17294-2 (Österreichisches Normungsinstitut, 2017).

A handheld XRF (X-ray fluorescence analysis, Bruker Magnum Metal-ceramic S1 Titan S/N: 600N3361) was used to determine the elemental composition of the precious metals fraction. Up to 100 particles were analysed, weighed and the composition was determined considering the masses of each analysed particle.

The residual fractions from XRF sorting were comminuted by a vibratory disc mill to <5 mm, subsequently rejuvenated, homogenised and digested with aqua regia (ÖNORM EN 13657(6.3), Österreichisches Normungsinstitut, 2002b). The dry substance was determined according to ÖNORM EN 14346 (Österreichisches Normungsinstitut, 2007) – procedure A. The samples were analysed for silver, gold, cobalt, chromium, copper, iron, manganese, niobium, nickel, lead, palladium, platinum, antimony, tin, vanadium and zinc using the ICP-MS screening method following ÖNORM EN ISO 17294-2 (Österreichisches Normungsinstitut,

2017). Molybdenum and tungsten were determined by inductively coupled plasma optical emission spectroscopy (ICP-OES, Varian Vista-MPX CCD) according to ÖNORM EN ISO 11885 (Österreichisches Normungsinstitut, 2009).

Calculations

The yields of XRF sorting and melting experiments were calculated according to equation (1) (R yield in wt%; M mass of desired or residual fraction from XRF sorting and of metal or slag from melting experiments, respectively, in kilograms; M_{input} input mass for XRF sorting and melting experiments, respectively, in kilograms):

$$R = \frac{M}{M_{input}} * 100 \quad (1)$$

The content of the elements i in the output fraction of XRF sorting and consequently the elemental composition of the desired fractions zinc, copper, brass and stainless steel were calculated based on the results of chemical analyses of metals and slags according to equation (2) (c_i content of element i in the desired fraction in per cent; R_m , R_s yield of metal and slag, respectively, in wt% during melting of the desired fraction; $c_{i,m}$, $c_{i,s}$ content of element i in the metal and in the slag, respectively, in wt%). The elementary contents c_i in the residual fractions were calculated from ICP-MS results, those in the precious metals fraction from XRF results (compare *Chemical analyses*):

$$c_i = \frac{R_m * c_{i,m} + R_s * c_{i,s}}{100} \quad (2)$$

To show the distribution of the elements copper, zinc, iron and lead across the XRF output fractions, equation (3) was used (R_i yield of element i in wt%; M mass of desired/residual fraction in kilograms; c_i content of element i in the desired/residual fraction in wt%; $M_{i,input}$ total mass of element i in the input of XRF sorting in kilograms):

$$R_i = \frac{M * c_i}{M_{i,input}} \quad (3)$$

Results and discussion

Mechanical processing

NF fractions for XRF sorting were produced by screening and the subsequent magnetic and eddy current separation. However, the NF fractions 6.3–10 mm and 10–16 mm had to be re-screened manually (analytical screens HAVER&BOECKER DIN ISO 3310-1, mesh size 5 mm and 10 mm) because too fine bottom ash particles for XRF sorting (minimum grain size 6 mm) were present in the products of mechanical processing as a result of the transport of the samples. Owing to manual screening, the mass losses are considered in further evaluations (6.3–10 mm: about 27 wt%, 10–16 mm: about 75 wt%). Re-screening of the fraction 16–20 mm was not necessary. The share of the NF fractions

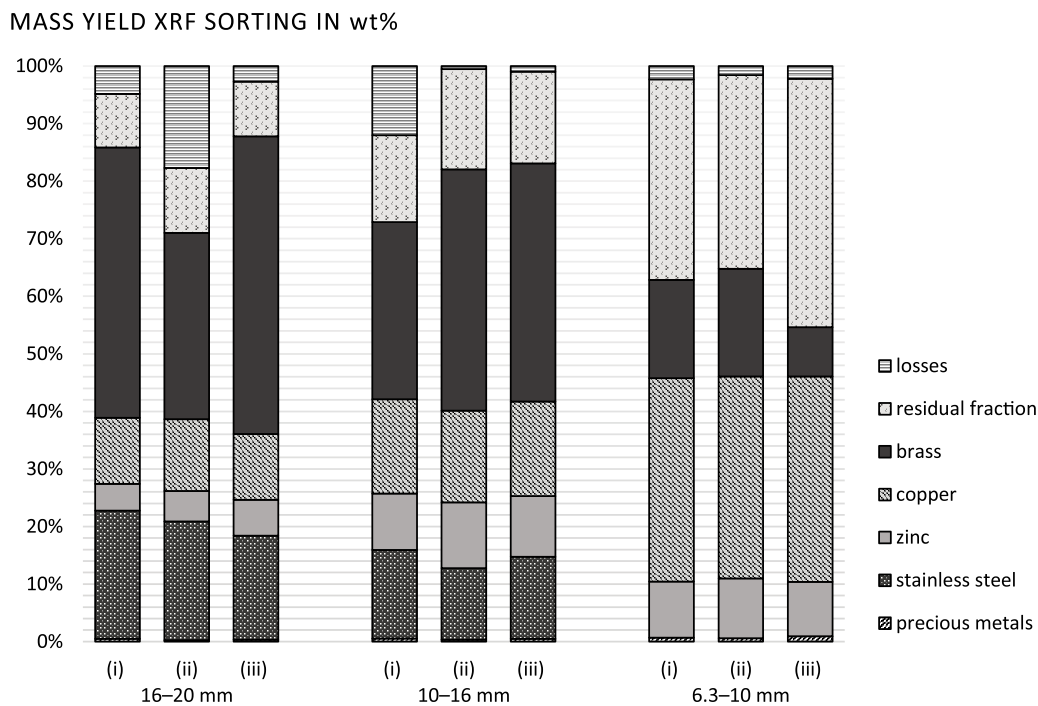


Figure 3. XRF sorting of the NF fractions 16–20, 10–16 and 6.3–10 mm – Yield for the experiments with (i) dry, (ii) wet and (iii) without surface treatment of the NF fractions.

6.3–20 mm on the fraction HNF metals 0–50 mm from the BWS process accounts for about 41 wt% (16–20 mm: 11 wt%, 10–16 mm: 17 wt%, 6.3–10 mm: 13 wt%). The content of ferrous metals accounted for about 16 wt% (16–20 mm: 5 wt%, 10–16 mm: 7 wt%, 6.3–10 mm: 4 wt%).

Surface pre-treatment and XRF sorting

Figure 3 illustrates the yield of the desired fractions precious metals, zinc, copper, brass and stainless steel of XRF sorting under consideration of the pre-treatment of the NF fractions, namely (i) drily pre-treated, (ii) wetly pre-treated and (iii) not pre-treated.

Whereas the yield of stainless steel and brass tends to increase with increasing grain size, the yield of zinc, copper and precious metals increases with decreasing grain size. The comparably large amounts of residual fractions in the grain size range 6.3–10 mm mainly result from the fact that no stainless steel was sorted out in the experiments. There is neither a positive nor a negative effect of pre-treatment on the yield of the desired fractions in XRF sorting. An exception is the brass fraction 16–20 mm, whose yield is reduced for increasing intensity of the pre-treatment. The mass losses across all sorted fractions were relatively low. They decrease proportionally with the grain size, explained partially by the fact that losses of smaller particles during the sorting process have smaller effects on the mass losses than losses of larger particles. For the differences between the various kinds of pre-treatment – (i) dry, (ii) wet or (iii) or no pre-treatment – no systematic correlation could be observed. Screening at a mesh size of 16 mm is not required

from a processing point of view as the ideal grain size range for sensor-based sorting is a ratio of 1:4 according to Bunge (2012). This is supported by the congruent results for the yield in the considered grain size ranges.

Figure 4 shows the elemental composition of the output fractions of XRF sorting in the grain size range 16–20 mm. No matter if the experiments were conducted with or without pre-treatment of the particle surface, all desired fractions have similar qualities. As the yield for stainless steel during re-melting of the drily pre-processed fraction exceeded 100% (see below) for the subsequent summary, a value of 100% was assumed.

Zinc: (i) 83.6% zinc (ii) 87.3% zinc (iii) 81.1% zinc

Copper: (i) 83.6% copper (ii) 86.2% copper (iii) 80.9% copper

Brass: (i) 58.3% copper; 33.0% zinc (ii) 56.0% copper; 34.7% zinc (iii) 56.9% copper; 33.4% zinc

Stainless steel: (i) 64.2% iron (ii) 63.6% iron (iii) 64.6% iron

Precious metals: (i) 18.0% silver (ii) 14.1% silver (iii) 12.6% silver

Copper, zinc, lead and iron were identified as the main constituents of the residual fraction for the three experiments (i)–(iii) (47.1–50.9% copper, 17.1–22.4% zinc, 7.9–10.0% lead and 1.1–2.7% iron).

The content of the elements copper and zinc (supposed to accumulate in the product fractions) in the residual fractions rises with increasing intensity of mechanical processing. This observation suggests decreased oxygen contents and consequently less oxide compounds in the residual fraction, if the bottom ash is

ELEMENTAL COMPOSITION IN wt% - XRF OUTPUT FRACTIONS

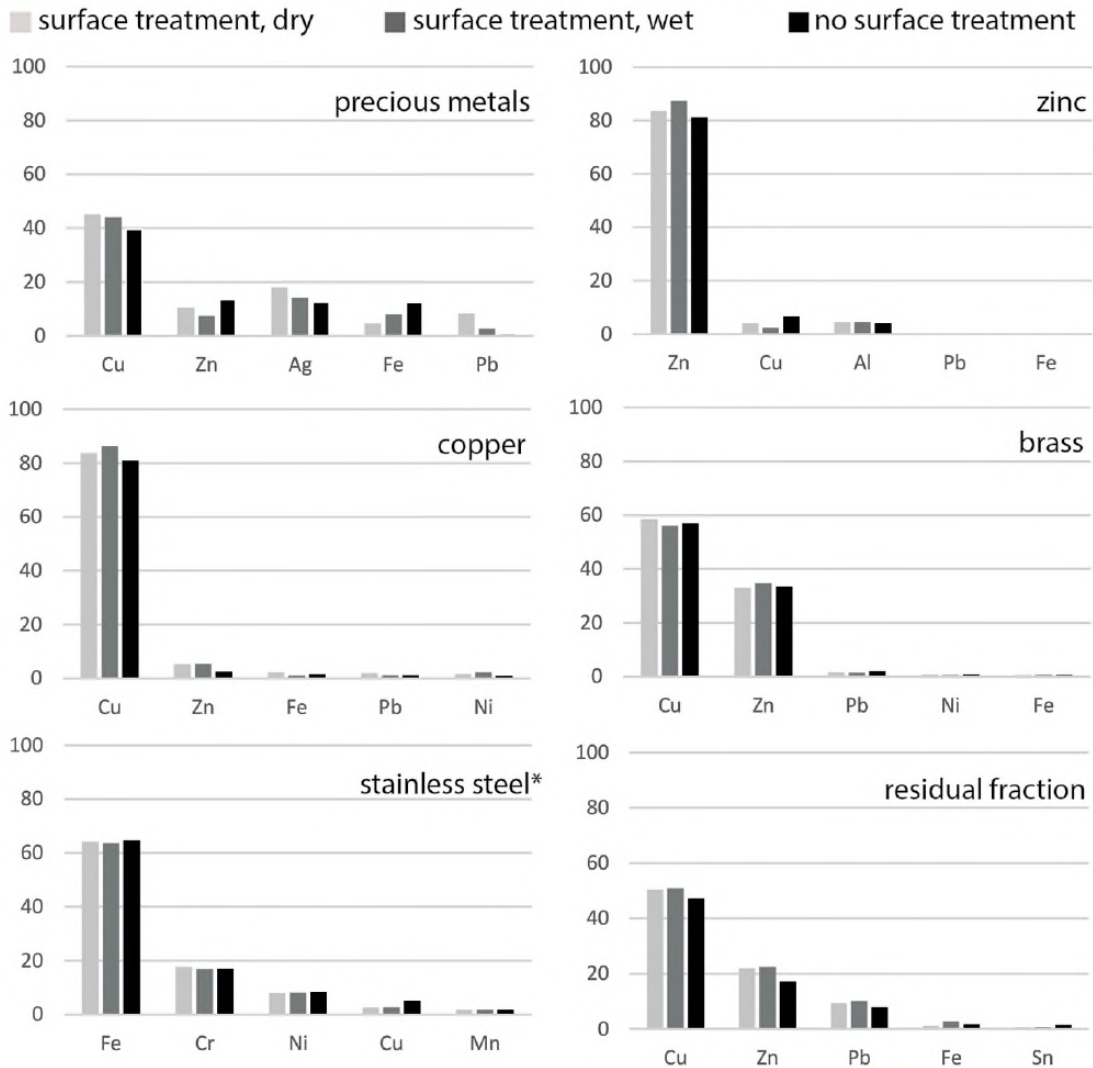


Figure 4. Elemental composition of the output fractions of XRF sorting experiments with (i) dry, (ii) wet and (iii) without surface treatment of the NF fractions 16–20 mm.

*The composition of the drily pre-treated stainless steel fraction (i) refers to a yield of $R_m = 100\%$.

pre-treated wetly or drily. Furthermore, this result suggests that by pre-treatment of the bottom ash corroded constituents, which are enriched in the slag during re-melting, are separated.

Figure 5 illustrates the distribution of the elements copper, zinc, iron and lead among the output flows of XRF sorting (grain size range 16–20 mm). Most of the copper from the input fractions is enriched in the copper and brass fractions (corresponds to $\leq 86.8\%$ of the entire copper contained in the input fractions). Up to 16.3% of the copper are lost with the residual fraction. Of the zinc contained in the input, 58.8% to 71.1% ends up in the brass fractions, 17.7% to 24.3% in the zinc fractions and 6.7% to 13.3% in the residual fractions. This is in general agreement with the statement of Bunge (2014), that zinc in pure form occurs in bottom ash only in minor amounts (0.2 wt%) and the majority is alloyed with copper as brass. The distribution of copper and zinc among the output flows of sensor-based sorting as well as the element composition of the output flows (see Figure 4), suggest that there is still optimisation potential regarding the yield of

brass, copper and zinc. Regarding an improvement or decline of the yield of copper and zinc depending on the pre-processing, no trend is visible. The majority of iron was yielded successfully into the stainless steel fraction ($>94.6\%$). Contrary, lead is enriched in the residual and brass fractions. Owing to the lead addition in copper–tin alloys, the lead content of the brass fraction is accordingly high (Deutsches Kupfer-Institut e.V., 2007). By the use of lead, the machinability of copper and copper alloys is improved (Deutsches Kupfer-Institut e.V., 2012).

Melting experiments

The achieved metal yield in melting experiments is 72%–84% for zinc, 73%–89% for copper, 60%–92% for brass and 92%–102% for stainless steel. The excess over 100% in the experiment with stainless steel can be explained by the uptake of carbon from the graphite crucible by the steel melt. The amount of volatilised elements that were separated in the condenser is zero for all

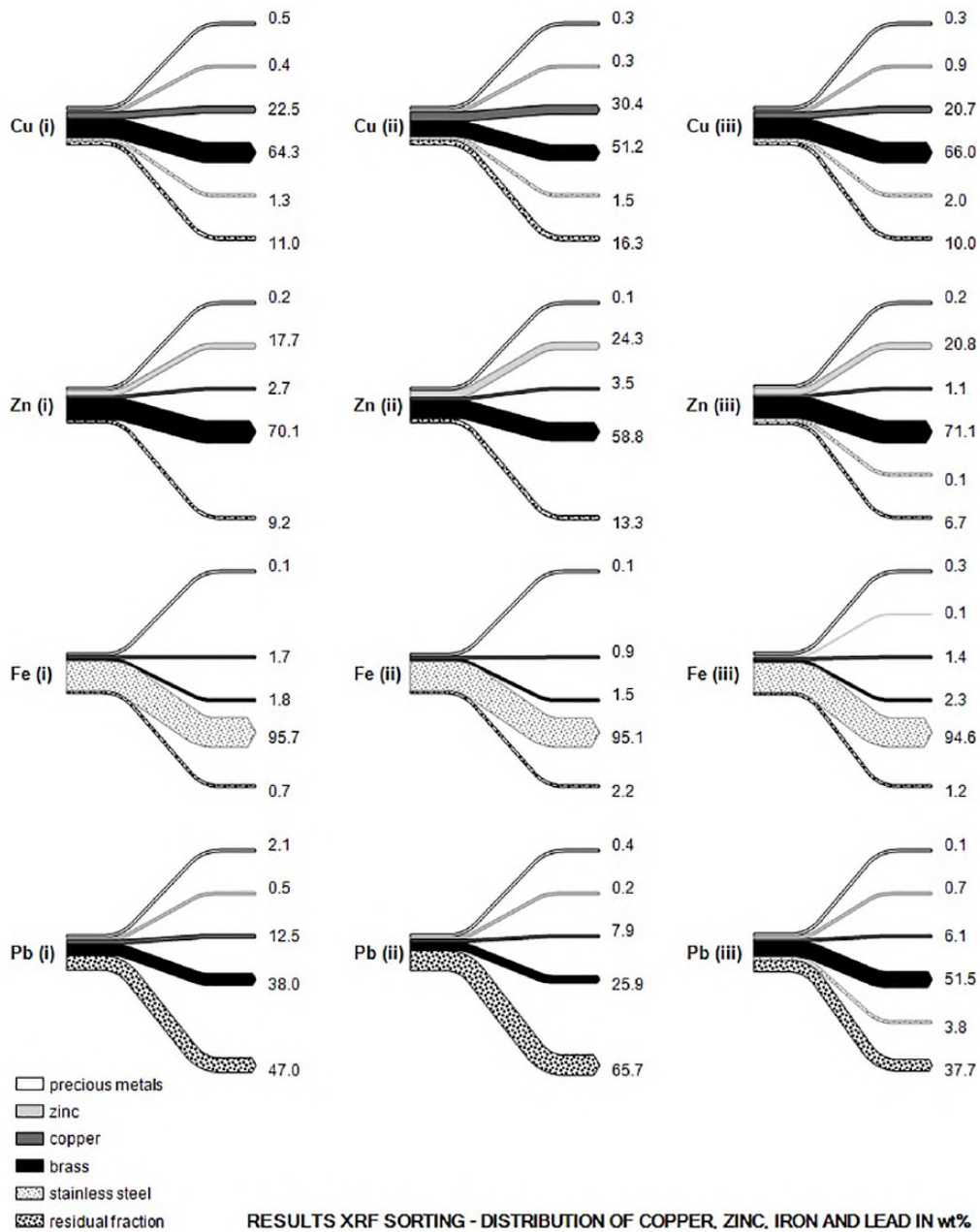


Figure 5. XRF sorting – Distribution of elements among the output fractions of XRF sorting in wt% ((i) surface treatment, dry, (ii) surface treatment, wet and (iii) no surface treatment).

fractions apart from those from the experiments with stainless steel. In the last case, metallic zinc sublimated because of the high temperatures. Owing to the oxygen in the atmosphere, zinc oxidised to ZnO and re-sublimated at the condenser. The losses are in the range of 1% to 8% (except for stainless steel where a weight increase of up to 4% was observed, see also the discussion of the yield). They can be traced back to metal residues on the skimmer or in the crucible. In case of the wetly pre-processed brass fraction and the wetly pre-processed stainless steel fraction, the experiments were conducted in triplicate owing to deviations between the results of the first two experiments to validate the results. Regarding the metal yield, no trend depending on the surface pre-treatment, for example (i) drily pre-treated, (ii) wetly pre-treated and (iii) not pre-treated, was recognised. Table 1

indicates the composition of the re-melted metals based on SEM/EDX investigations. The results from SEM/EDX and OES agree with each other. However, for the zinc samples, copper, lead and aluminium were outside the calibration range of the OES measurement. For the stainless steel samples, this affected partly the lead and carbon contents.

The re-melted zinc fraction contains between 86.8% and 91.4% zinc. The main alloying element is aluminium, with up to 4.8%. The copper content varies considerably within the individual fractions with identical pre-treatment. Overall, the content of accompanying elements does not depend on the kind of pre-treatment. In Germany, hard zinc as well as zinc top and bottom drosses from galvanisation industry with zinc contents >90% are used for the production of zinc oxide (Th, 2016). Hence, the

Table 1. Excerpt – Composition of the re-melted metals zinc, copper, brass and lead (SEM/EDX, (i) surface treatment, dry, (ii) surface treatment, wet, (iii) no surface treatment). Remark: Each sample was analysed three times and thereof the mean μ and the standard deviation σ was calculated. Values below the quantification limit (<0.1 wt%) are shown as ‘—’.

			Cu	Zn	Fe	Ni	Pb	Sn	C	O	Cr	Mn	Al
Zinc	(i)	μ	2.7	90.2	—	—	—	—	0.8	1.3	—	—	4.8
		σ	0	0.3	—	—	—	—	0.4	0.1	—	—	0.2
	(i)	μ	4.9	87.3	—	0.1	—	—	1.2	1.8	—	—	4.7
		σ	0.2	0.1	—	0.2	—	—	0.1	0	—	—	0
	(ii)	μ	2.2	91.4	—	—	—	—	0.5	1.2	—	—	4.6
		σ	0.1	0.1	—	—	—	—	0.1	0.1	—	—	0.2
	(ii)	μ	3.7	88.1	—	0.1	1	—	1	1.3	—	—	4.8
		σ	0	0.6	—	0.2	0.1	—	0.4	0.1	—	—	0.1
	(iii)	μ	2.4	90.6	—	—	—	—	1	1.4	—	—	4.6
		σ	0	0.2	—	—	—	—	0.2	0.2	—	—	0.1
	(iii)	μ	6.4	86.8	—	—	—	—	0.8	1.2	—	—	4.7
		σ	0.1	0.1	—	—	—	—	0.1	0	—	—	0.1
Copper	(i)	μ	88.7	5.5	0.8	1.7	1.5	0.7	0.3	0.4	—	—	0.3
		σ	0.3	0.1	0	0	0.2	0.1	0.1	0.4	—	—	0
	(i)	μ	89.1	5.1	0.6	2.2	0.8	0.6	0.6	0.6	—	—	0.4
		σ	0.9	0.2	0	0.1	0.1	0.1	0.7	0.1	—	—	0.1
	(ii)	μ	88.8	5.4	0.7	2.4	1.1	0.5	0.2	0.5	—	—	0.4
		σ	0.2	0.1	0	0.1	0.1	0.1	0.1	0.1	—	—	0.1
	(ii)	μ	86.7	7.6	0.5	3.1	0.4	0.5	0.3	0.5	—	—	0.4
		σ	0.3	0.2	0	0	0.4	0.1	0.1	0.4	—	—	0.1
	(iii)	μ	90.3	2.6	0.9	1	1.2	0.4	2.6	0.7	—	—	—
		σ	3.4	0.1	0	0.1	0.1	0.1	2.7	0.2	—	—	—
	(iii)	μ	88.9	5.3	0.4	2.4	0.8	0.7	0.4	0.6	—	—	0.4
		σ	0.1	0.1	0	0	0.2	0.1	0.2	0	—	—	0
Brass	(i)	μ	62.5	31.9	0.4	0.8	1.6	0.5	1.4	0.7	—	—	—
		σ	0.3	0.3	0	0	0	0	0	0	—	—	—
	(i)	μ	61.9	32.2	0.4	0.7	1.5	0.4	1.9	0.7	—	—	0.1
		σ	0.3	0.3	0	0	0.2	0	0.3	0.1	—	—	0.2
	(ii)	μ	61.7	34	0.3	0.6	1.5	0.4	0.8	0.6	—	—	—
		σ	0.3	0.6	0	0	0.1	0	0.3	0	—	—	—
	(ii)	μ	60.9	33.6	0.4	0.3	1.7	0.4	1.8	0.8	—	—	—
		σ	0.4	0.3	0	0.3	0.2	0	0.5	0	—	—	—
	(ii)	μ	62	31.5	0.4	0.7	1.6	0.5	2.4	0.7	—	—	—
		σ	0.4	0.1	0	0	0.1	0.1	0.4	0	—	—	—
	(iii)	μ	60.6	33.1	0.3	0.8	2.1	0.4	1.7	0.7	—	—	—
		σ	0.4	0.2	0	0.1	0.1	0.1	0.2	0.1	—	—	—
(iii)	μ	60.8	32.4	0.4	0.4	2.1	0.3	2.8	0.6	—	—	—	
	σ	0.3	0.1	0	0.4	0.2	0	0.3	0	—	—	—	
Stainless steel	(i)	μ	2.5	—	64.2	7.9	—	—	5	—	17.6	1.6	—
		σ	0.1	—	0.5	0.1	—	—	0.3	—	0.6	0.1	—
	(i)	μ	1.2	—	64.2	8.1	—	—	6.2	—	17.2	1.4	0.2
		σ	0.1	—	0.4	0.1	—	—	0.4	—	0.2	0.1	0
	(ii)	μ	2.6	—	63.9	8.1	—	—	4.9	—	17	1.7	0.3
		σ	0.1	—	0.5	0.2	—	—	0.6	—	0.1	0	0
	(ii)	μ	1.4	—	64.9	7.6	—	—	5.5	—	16.8	2.2	0.2
		σ	0.1	—	0.3	0.2	—	—	0.6	—	0.1	0.1	0
	(ii)	μ	3.8	—	65.1	8.5	—	—	1.4	—	17	2.3	0.6
		σ	0.2	—	0.2	0.2	—	—	0.2	—	0.3	0.1	0
	(iii)	μ	4.1	—	66.5	8.7	—	—	0.3	—	17.6	1.7	—
		σ	0.2	—	0.4	0.2	—	—	0.4	—	0.3	0.1	—
(iii)	μ	3.8	—	62.5	7.7	—	—	5.2	—	16.5	2.2	—	
	σ	0.1	—	0.4	0.3	—	—	0.3	—	0.1	0.1	—	

recycling of the zinc fractions produced in this project seems realistic, for example by the French process (Worrell and Reuter, 2014). Furthermore, electric arc furnace dusts with 40% zinc can

be recycled pyrometallurgically (Lin et al., 2017). Aluminium (3.8%–4.2%) and copper (0.7%–1.1% in case of the Zamak alloy ZL0410) are used as alloying elements for casting alloys.

Aluminium improves for example the processability, tensile strength, fracture elongation and impact bending toughness of zinc, whereas copper has a positive impact on the tensile strength and hardness of the metal (Röhr, 2017). However, the quality requirements according to ÖNORM EN 13283 (Österreichisches Normungsinstitut, 2003) for secondary zinc (>97.5% for quality ZS2) and according to ÖNORM EN 1774 (Österreichisches Normungsinstitut, 1997) for casting alloys (sort-specific, very strict limit values for accompanying elements) are not reached.

The main constituent of the copper fractions is copper (86.7%–90.3%). The main accompanying elements are zinc and nickel. Additionally, lead, iron and zinc were identified as accompanying elements. In contrast, the concentration of single alloying elements in low-alloy copper material is limited to a percentage of 1%–2%, in total 5% (Deutsches Kupfer-Institut e.V., 2012). Corresponding refining steps would be necessary to increase the electrical conductivity for electric and electronic applications (Deutsches Kupfer-Institut e.V., 2000).

The brass blocks produced in the melting experiments consist mainly of two parts of copper and one part of zinc (copper: 60.6%–62.5%, zinc: 31.9%–33.6%). According to the German Copper Institute (Deutsches Kupfer-Institut e.V., 2007) common copper–zinc alloys contain, besides copper, also 5 to 45 wt% zinc.

The iron contents of the stainless steel fraction range from 62.5 wt% to 66.5 wt%. The main alloying element is chromium with 16.5–17.6 wt% followed by nickel with 7.6–8.7 wt%. Manganese is present with about 2 wt%. Iron alloys with $\geq 10.5\%$ chromium and $\leq 1.2\%$ carbon belong to the group of stainless steel (Informationsstelle Edelstahl Rostfrei, 2008). Owing to the high temperatures and erosion of carbon crucible by stirring of melt, carbon is dissolved in the steel melt. With decreasing temperature during solidification, the solubility of carbon significantly decreases resulting in a large number of carbides formed in the material. Consequently, the carbon content rises to 6.2 wt%. In the case of stainless steels, chromium carbides preferentially form, which lead to a decrease of corrosion resistance. Besides, the materials embrittle and the weldability sinks (Angerer N.D.; Kinzel, 1952).

The composition of all re-melted samples corresponds to the respective desired fractions from XRF sorting. Only the contained lead has to be removed to obtain better saleable products. The maximum allowed concentration for lead for homogeneous materials is 0.1 wt% according to article 4 of the European guideline 2011/65/EU (The European Parliament and the Council of the European Union, 2011). The surface pre-treatment has no impact on the purity and the composition of the products from melting experiments. The slags from the experiments are no homogeneous liquid phases, but crumbly to doughy surface layers.

Summary

In this study, mixed non-ferrous metals fractions from wet processing of MSWI bottom ash, which are currently directly

recycled metallurgically, are further separated mechanically to recover besides copper also brass, zinc, stainless steel and precious metals.

The conducted experiments demonstrate that zinc, copper, brass, stainless steel and precious metals fractions can be produced in a marketable quality by XRF sorting. Neither a positive nor a negative effect of surface pre-treatment (wet, dry) on the purity of the desired fractions could be proven. Only the yield of the brass fraction in the grain size range 16–20 mm decreased with increasing mechanical treatment intensity.

Regarding the metal yield and the quality of the re-melted metals, the surface cleaning of the particles prior to XRF sorting had no effect. The produced melt products had marketable qualities (zinc: 86.8–91.4% zinc; copper: 86.7–90.3% copper; brass: 60.6–62.5% copper and 31.5–34.0% zinc; stainless steel: 62.5–66.5% iron).

In order to obtain better saleable products (metals and alloys), it is recommended to separate the lead contained in the re-melted fractions, which could be achieved by an additional XRF sorting step (depending on whether the lead in the non-ferrous bottom ash is present as metal or alloy and the related mass distribution). In addition, further pyrometallurgical and hydrometallurgical processes could be used to refine the products and to lower lead contents in the re-melted fractions, respectively. However, further experiments have to be performed to make reliable scientific statements.

Acknowledgements

The authors thank the Austrian Research Promotion Agency (FFG) for funding the project, as well as all contributing research and industrial partners and Alexia Aldrian (Montanuniversität Leoben) and her team for the chemical analyses.


Declaration of conflicting interests


The authors declared no potential conflicts of interest with respect to the research, authorship, and/or publication of this article.

Funding

The authors disclosed receipt of the following financial support for the research, authorship, and/or publication of this article: The authors thank the Austrian Research Promotion Agency (FFG) for funding the project AKRosA II [No. 848621].

ORCID iDs

Kerstin Pfandl  <https://orcid.org/0000-0002-8103-4784>

Bastian Küppers  <https://orcid.org/0000-0002-0367-4786>

References

- Allegrini E, Maresca A, Olsson ME, et al. (2014) Quantification of the resource recovery potential of municipal solid waste incineration bottom ashes. *Waste Management* 34: 1627–1636.
- Angerer M (N.D.) Stahl – Einfluss der Legierungselemente. Available at: <http://www.maschinenbau-wissen.de/skript3/werkstofftechnik/stahl-eisen/38-einfluss-legierungselemente-stahl> (accessed 22 July 2019).
- Bayuseno AP and Schmah WW (2010) Understanding the chemical and mineralogical properties of the inorganic portion of MSWI bottom ash. *Waste Management* 30: 1509–1520.

- BOKU (2010) Institut für Abfallwirtschaft, Universität für Bodenkultur Wien. Grundlagen für die Verwertung von MV-Rostasche: Teil A: Entwicklung des Österreichischen Behandlungsgrundsatzes. Available at: https://www.bmmt.gv.at/dam/jcr:3e990e78-f77d-4d52-b9a1-b3b5ffe5630a/BOKU_Grundsatz_Teil_A_Rostasche.pdf+&cd=1&hl=de&ct=clnk&gl=at&client=firefox-b-d (accessed 23 July 2019).
- Bundesministerium für Verkehr, Innovation und Technologie (2018) Definition: Kritische Rohstoffe und potenziell kritische Rohstoffe mit Bezug zu Österreich. Available at: https://www.ffg.at/sites/default/files/allgemeine_downloads/thematische%20programme/Produktion/rohstoffdefinition_28as_pdz_2018.pdf (accessed 25 March 2019).
- Bunge R (2012) *Mechanische Aufbereitung: Primär- und Sekundärrohstoffe*, 1st edn. Weinheim, Germany: Wiley-VCH Verlag & Co. KGaA, pp.206.
- Bunge R (2014) Wieviel Metall steckt im Abfall? In: Thomé-Kozmiensky KJ (ed.) *Mineralische Nebenprodukte und Abfälle*, Neuruppin, DE: TK Verlag Karl Thomé-Kozmiensky, pp.91–103.
- Bunge R (2016) Aufbereitung von Abfallverbrennungssaschen – eine Übersicht. In: Thomé-Kozmiensky KJ (ed.) *Mineralische Nebenprodukte und Abfälle*, vol 3. Neuruppin, DE: TK Verlag Karl Thomé-Kozmiensky, pp.141–161.
- Dittrich S, Thome V, Seifert S, et al. (2016) Effektive Aufbereitung von Müllverbrennungsschlacken mittels Hochspannungsimpulsen. *Chemie Ingenieur Technik* 88: 461–468.
- Deutsches Kupfer-Institut e.V. (2000) Kupfer in der Elektrotechnik – Kabel und Leitungen. Available at: https://www.kupferinstitut.de/fileadmin/user_upload/kupferinstitut.de/de/Documents/Shop/Verlag/Downloads/Anwendung/Elektrotechnik/brosch09.pdf (accessed 15 March 2019).
- Deutsches Kupfer-Institut e.V. (2007) Kupfer-Zink-Legierungen (Messing und Sondermessing). Available at: https://www.kupferinstitut.de/fileadmin/user_upload/kupferinstitut.de/de/Documents/Shop/Verlag/Downloads/Werkstoffe/i005.pdf (accessed 22 March 2019).
- Deutsches Kupfer-Institut e.V. (2012) Niedriglegierte Kupferwerkstoffe: Eigenschaften Verarbeitung Verwendung. Available at: https://www.kupferinstitut.de/fileadmin/user_upload/kupferinstitut.de/de/Documents/Shop/Verlag/Downloads/Werkstoffe/i008.pdf (accessed 11 March 2019).
- European Commission (2017) Study on the review of the list of critical raw materials: Final report. Available at: <http://hytechcycling.eu/wp-content/uploads/Study-on-the-review-of-the-list-of-Critical-Raw-Materials.pdf> (accessed 13 June 2019).
- ecoprog GmbH (2018) Dynamic development of waste-to-energy market continues. Available at: https://www.ecoprog.com/fileadmin/user_upload/pressemitteilungen/ecoprog_press_release_Waste_to_Energy_2017-2018.pdf (accessed 13 June 2019).
- Funari V, Braga R, Bokhari SNH, et al. (2015) Solid residues from Italian municipal solid waste incinerators: A source for “critical” raw materials. *Waste Management* 45: 206–216.
- Gillner R, Pretz T, Rombach E, et al. (2011) NE-Metallpotenzial in Rostaschen aus Müllverbrennungsanlagen. *Word of Metallurgy – ERZMETALL* 64: 5–13.
- Gisbertz K and Friedrich B (2015) VeMRec – Metallurgische Herausforderungen beim Recycling von NE-Metallkonzentraten aus Abfallverbrennungs-Rostasche. In: Thomé-Kozmiensky KJ (ed.) *Mineralische Nebenprodukte und Abfälle*. Neuruppin, DE: TK Verlag Karl Thomé-Kozmiensky, pp.227–253.
- Informationsstelle Edelstahl Rostfrei (2008) Merkblatt 803: Was ist nichtrostender Stahl? Available at: <https://www.edelstahl-rostofffrei.de/page.asp?pageID=1576> (accessed 26 June 2019).
- Johnson A and Huter C (2010) Characterization and geochemical properties of selected incineration residues. In: Schenk K (ed.) *KVA-Rückstände in der Schweiz: Der Rohstoff mit Mehrwert*. Bern: Bundesamt für Umwelt, pp.145–151.
- Jung C-H and Osako M (2007) Thermodynamic behavior of rare metals in the melting process of municipal solid waste (MSW) incineration residues. *Chemosphere* 69: 279–288.
- Kinzel AB (1952) Chromium carbide in stainless steel. *JOM* 4: 469–448.
- Kollegger P and Berghofer M (2017) Optimierte sensorgestützte Mineraliensortierung durch mineralogisch-petrographische Prozesskontrolle. *Berg Huettenmaennische Monatshefte* 162: 457–459.
- Kranert M and Cord-Landwehr K (eds) (2010) *Einführung in die Abfallwirtschaft*, 4th edn, updated and expanded. Wiesbaden, Germany: Vieweg und Teubner Verlag, pp.316–117.
- Lin X, Peng Z, Yan J, et al. (2017) Pyrometallurgical recycling of electric arc furnace dust. *Journal of Cleaner Production* 149: 1079–1100.
- Österreichisches Normungsinstitut (1997) ÖNORM EN 1774 Zink und Zinklegierungen – In Blockform und in flüssiger Form.
- Österreichisches Normungsinstitut (2002a) ÖNORM EN 13656 Charakterisierung von Abfällen – Aufschluss mittels Mikrowellengerät mit einem Gemisch aus Fluorwasserstoffsäure (HF), Salpetersäure (HNO₃) und Salzsäure (HCl) für die anschließende Bestimmung der Elemente im Abfall.
- Österreichisches Normungsinstitut (2002b) ÖNORM EN 13657 Charakterisierung von Abfällen – Aufschluss zur anschließenden Bestimmung des in Königwasser löslichen Anteils an Elementen in Abfällen.
- Österreichisches Normungsinstitut (2003) ÖNORM EN 13283 Zink und Zinklegierungen – Sekundärzink.
- Österreichisches Normungsinstitut (2007) ÖNORM EN 14346 Charakterisierung von Abfällen – Berechnung der Trockenmasse durch Bestimmung des Trockenrückstandes oder des Wassergehaltes.
- Österreichisches Normungsinstitut (2009) ÖNORM EN ISO 11885 Wasserbeschaffenheit – Bestimmung von ausgewählten Elementen durch induktiv gekoppelte Plasma-Atom-Emissionsspektrometrie (ICP-OES).
- Österreichisches Normungsinstitut (2011) ÖNORM S 2127 Grundlegende Charakterisierung von Abfallhaufen oder von festen Abfällen aus Behältnissen und Transportfahrzeugen.
- Österreichisches Normungsinstitut (2017) ÖNORM EN ISO 17294-2 Wasserbeschaffenheit – Anwendung der induktiv gekoppelten Plasma-Massenspektrometrie (ICP-MS) Teil 2: Bestimmung von ausgewählten Elementen einschließlich Uran-Isotope.
- Pan JR, Huang C, Kuo J-J, et al. (2008) Recycling MSWI bottom and fly ash as raw materials for Portland cement. *Waste Management* 28: 1113–1118.
- Pfandl K, Dobra T and Pomberger R (2018) Potential von Müllverbrennungsrostaschen für die Rückgewinnung kritischer Rohstoffe. In: Bockreis A, Faulstich M, Flamme S, et al. (eds) *8. Wissenschaftskongress Abfall- und Ressourcenwirtschaft*, 15–16 March, Universität für Bodenkultur (BOKU) Wien, Austria, 1st edn. Innsbruck, AT: Innsbruck University Press pp.245–252.
- Röhr G (2017) Zinklegierungen – genormte Qualität aus primären und sekundären Rohstoffen. In: Verband Deutscher Metallhändler e.V. (ed.) *VDM Magazin II/2017 (675)*, pp.10–11.
- Simon F-G and Holm O (2013) Aufschluss, Trennung und Rückgewinnung von Metallen aus Rückständen thermischer Prozesse: Verdoppelung der Metallausbeute aus MVA-Rostasche. In: Thomé-Kozmiensky KJ (ed.) *Aschen, Schlacken, Stäube: Aus Abfallverbrennung und Metallurgie*. Neuruppin, DE: TK Verlag Karl Thomé-Kozmiensky, pp.297–310.
- Stockinger G (2016) Innovative Aufbereitung von Müllverbrennungsschlacke. In: Pomberger R, Adam J, Aldrian A, et al. (eds) *Recy & DepoTech 2016*, 8–11 November, Montanuniversität Leoben. Austria, Leoben, AT: self-published by AVAW, pp.237–242.
- Th (2016) Zinkverbindungen aus Recycling-Rohstoffen: Erfolgreiche Kreislaufwirtschaft bei der Zinkgewinnung. Available at: <https://www.giesserei-praxis.de/news/news/14822-zinkverbindungen-aus-recycling-rohstoffen/> (accessed 22 July 2019).
- The European Parliament and the Council of the European Union (2011) DIRECTIVE 2011/65/EU OF THE EUROPEAN PARLIAMENT AND OF THE COUNCIL: of 8 June 2011 on the restriction of the use of certain hazardous substances in electrical and electronic equipment. Available at: <https://eur-lex.europa.eu/legal-content/EN/TXT/PDF/?uri=CELEX:32011L0065&from=DE> (accessed 4 July 2019).
- Wang Y, Huang L and Lau R (2016) Conversion of municipal solid waste incineration bottom ash to sorbent material: Effect of ash particle size. *Journal of the Taiwan Institute of Chemical Engineers* 68: 351–359.
- Worrell E and Reuter MA (eds.) (2014) *Handbook of Recycling: State-of-the-Art for Practitioners, Analysts, and Scientists*. Amsterdam, Boston, Heidelberg, London, New York, Oxford, Paris, San Diego, San Francisco, Sydney, Tokyo: Elsevier, pp.133–124.
- Zhang F-S, Yamasaki S and Kimura K (2001) Rare earth element content in various waste ashes and the potential risk to Japanese soils. *Environment International* 27: 393–398.